

Microscopic Structures of the Negative Cluster in Crystalline Si

Toru Akiyama and Atsushi Oshiyama

Institute of Physics, University of Tsukuba, 1-1-1 Tennodai, Tsukuba 305-8571, Japan
 Fax: +81-0298-53-4492, e-mail: akiyama@cm.ph.tsukuba.ac.jp

We study geometric and electronic structures of Si negative clusters and their capability of containing impurities using total-energy electronic-structure calculations in the density functional theory. We find the magic numbers of the negative clusters are 6 (hexavacancy) and 10 (decavacancy) within the accuracy of density functional theory. We also find these negative clusters are capable of containing impurities such as hydrogen and oxygen, and form some complexes. Comparison of calculated local vibration modes with experiments allows us to identify these clusters.

Key words: negative cluster, silicon, magic numbers, density functional theory

1. INTRODUCTION

Vacancies in Si affect crucially the properties of host material, and play roles in a variety of aspects. The electronic and structural properties of single vacancy V_1 (monovacancy) and double vacancy V_2 (divacancy) have been identified both from experiments^{1,2)} and theoretical calculations³⁾. However, the identification for vacancy aggregates has been less pursued compared with the case of V_1 and V_2 . Since these aggregates can be regarded as negative clusters in materials, they are expected to have stable sizes and structures (magic numbers). The magic numbers of these clusters have been predicted theoretically by Chadi and Chang based on a simple dangling bond counting model⁴⁾. However, electronic structures of the negative clusters have not been revealed. In addition, the negative clusters can serve as a container of impurities and become decisive to the properties. Recently, in Si^+ ions implanted Si, hydrogen molecule which is considered to come in the vacancy aggregate was observed by a Raman experiment⁵⁾: the vibration frequencies of H_2 is in between the frequency of H_2 in the gas phase and at the interstitial site. It is thus likely that the negative cluster interacts with impurities and form some complexes.

In the present work, we investigate geometric and electronic structures of Si negative clusters based on the total-energy electronic-structure calculation using the local density approximation (LDA) or the generalized gradient approximation (GGA) in the framework of density functional theory. The magic numbers of the negative clusters are found to be 6 (hexavacancy) and 10 (decavacancy) within the accuracy of density functional theory. We find peculiar features in effects of lattice relaxation and electronic structures of these stable clusters. We also find that negative clusters are capable of containing impurities such as hydrogen and oxygen. Comparisons of calculated local vibration modes and infrared(IR) absorption

or Raman scattering experiments are made in order to identifying these complexes.

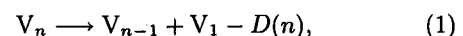
2. CALCULATION METHOD

All calculations have been performed using the LDA⁶⁾ or the GGA⁷⁾ in density functional theory⁸⁾. We use norm-conserving pseudopotential⁹⁾ for Si and H atoms, and ultrasoft pseudopotential¹⁰⁾ for O atoms. The conjugate-gradient minimization technique is applied both for ionic and electronic degrees of freedom¹¹⁾. The vacancy in an otherwise perfect crystal is simulated by a supercell. We find that the 64-site supercell is enough for the small vacancy V_n ($n \leq 7$) and the 216-site supercell is necessary for the large vacancy ($n \geq 8$) to obtain sufficiently accurate formation energies. We use the Γ -point sampling in the Brillouin zone integration, and the plane-wave basis set with a cutoff energy of typically 14Ry¹²⁾. Geometries are fully optimized for all atoms until the remaining force on each atom is less than 0.004 Ry/Å.

3. RESULTS AND DISCUSSION

3.1 Structures of the negative clusters

We first investigate the geometric and electronic structures of pristine negative clusters. The stable sizes and structures of the negative clusters V_n are assessed by using its formation energy $E_f(n)$. When we consider a dissociation reaction,



the dissociation energy $D(n) \equiv E_f(n-1) + E_f(1) - E_f(n)$ is a measure of the stability of V_n . The value of $D(n)$ defined above becomes large positive for the stable negative clusters. Figure 1 shows calculated $D(n)$ as a function of the size of the negative clusters. It is clear that $D(n)$ becomes positively large: The closed hexagonal-shape V_6 (Fig. 2(a)) and the adamantine-shape

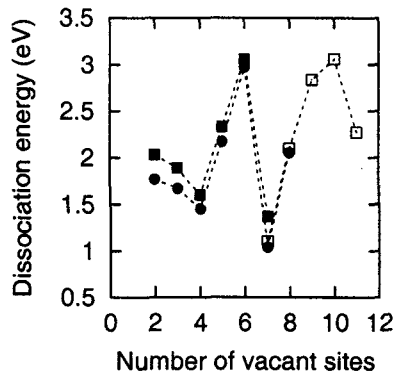


Figure 1: Calculated dissociation energy $D(n)$ as a function of the size of the negative cluster V_n obtained by the LDA with the 64-site supercell (circles), or by the GGA with either the 64- (solid squares) or the 216-site (open squares) supercell. Lines are guides for eyes.

V_{10} (Fig. 2(b)) are stable Si negative clusters, indicating that 6 and 10 are the magic numbers.

Lattice relaxation of neighboring atoms and the electronic structure of for stable V_6 are unusual. In V_6 , as shown in Fig. 2(a), each 2 nearest-neighbor atoms belonging to one vacant site are distorted to form a pair. The length of the bond due to the pairing is 2.86 Å (20% longer than the bulk bond length) in the GGA with the 216-site supercell. This pairing distortion, which keeps the threefold symmetry of the unrelaxed V_6 , makes 12 dangling bond states become 6 bonding and 6 antibonding states of the paired rebonds. Analysis of the calculated wave functions leads to a conclusion that the bonding states are resonant in the valence bands and that 4 antibonding states appear in the energy gap with 0.3 ~ 0.1 eV below the conduction band bottom.

In the optimized geometry of V_{10} , as shown in Fig. 2(b), 12 of 16 nearest neighbors are rebonded. The bond length is 2.80 Å in the GGA with the 216-site supercell. Yet even after relaxation there remain 4 nearest neighbor Si atoms which are separated by 7.93 Å from each other. We find that this causes dangling bonds, which induce a single deep level (a_1 state) and an almost triply degenerate level (t_2 state) at 0.16 eV and 0.29 eV, respectively, above the top of valence band. It is of interest that the T_d symmetry of the unrelaxed V_{10} is almost kept even after the relaxation: we are unable to recognize symmetry-lowering (Jahn-Teller) distortions in the present calculation, although the triply degenerated level is (partially) occupied by 2 electrons for neutral charge state. Due to the substantial separation of these dangling bonds in V_{10} , it seems that little electronic energy is gained by Jahn-Teller distortion. This peculiar electronic structure in V_{10} implies a possibility of spin polarization instead of

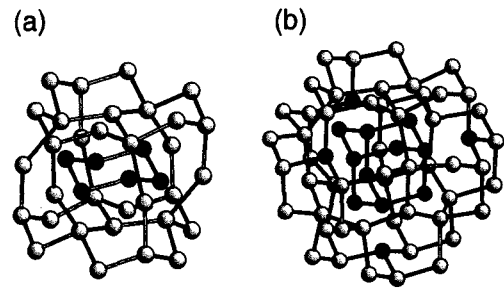


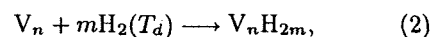
Figure 2: Atomic configurations of surrounding atoms of vacant site for relaxed (a) V_6 and (b) V_{10} . White and black circles represent Si atoms and vacant sites, respectively. Four nearest neighbor atoms each of which does not have any atom to form a pair are represented by the shaded circles.

Jahn-Teller distortion.

Thus, we investigate the geometric and electronic structures of V_{10} taking account of the spin polarization of electrons. We find that for the most stable structure (the formation energy is 12.27 eV) the electron spin is polarized: the number of polarized spin is 4.0. The energy of spin unpolarized structure is higher than this most stable structure by 0.44 eV. We also investigated the feasibility of charged V_{10} . Fig. 3 shows the calculated formation energies as a function of electron chemical potential μ_e . Here, zero of μ_e is taken to be the energy of the top of the valence band. We find that the neutral V_{10} is stable for low μ_e ($\mu_e \leq 0.27$ eV), and a transition from the neutral V_{10} to the doubly negative decavacancy V_{10}^{2-} occurs when μ_e exceeds 0.27 eV. In V_{10}^{2-} , the number of polarized spin is 2.0. The V_{10}^{2-} is found to be stable in the range of $0.27 \leq \mu_e \leq 0.67$ eV. The quadruply negative decavacancy V_{10}^{4-} is stable when μ_e exceeds 0.67 eV. However, the electron spins are unpolarized in this vacancy. Neither singly positive decavacancy V_{10}^+ , singly negative decavacancy V_{10}^- , nor triply negative decavacancy V_{10}^{3-} is stable at any point in the band gap. This indicates that the V_{10} has a *negative-U* character³⁾.

3.2 Hydrogen incorporation

Next, we consider hydrogen incorporation of the vacancies. We calculate the energy gain of the reaction where all the dangling bonds of the vacancies are terminated by hydrogen atoms:



where $H_2(T_d)$ indicates the hydrogen molecule at the T_d site. It is found that this reaction is exothermic (The reaction energies are found to

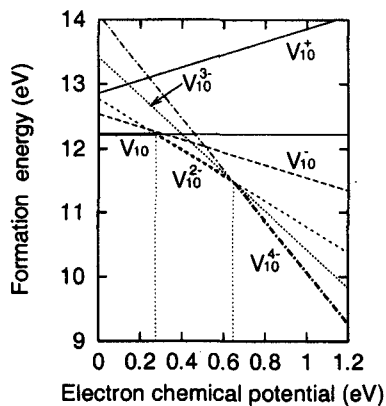
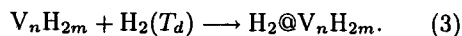


Figure 3: Calculated formation energy of V_{10} as a function of electron chemical potential μ_e . The vertical dashed lines indicate the transition levels. The stable charge state for each μ_e is emphasized.

be 4.3~19.8 eV for $n=1\cdots,6,10$). We also consider the trapping of the hydrogen molecule by the hydrogenated vacancies:



It is found that this reaction is also exothermic: The gained energies are found to be 0.15~1.1 eV for $n=1\cdots,6,10$. We then expect that hydrogen molecules trapped in hydrogen decorated vacancies are actually observed under some condition and thus calculate vibration frequencies of the molecules. In the calculation, anharmonic effects are fully considered by the 4-th order polynomial expansion. Table I shows the calculated bond length and stretching frequencies of an H_2 in these hydrogen decorated vacancies. It is found that the anharmonic parts are extremely important for hydrogen-related normal modes. From the calculated frequencies of H_2 it is confirmed that the peak¹³⁾ at 3618 cm^{-1} is due to H_2 at T_d . In V_1 and V_2 , we find the systematic increase on frequencies with increasing size of the hydrogen decorated vacancy. However, the frequency of an H_2 in $V_6 H_{12}$ already saturates. Moreover, it is reasonable to conclude that the newly observed peak⁵⁾ at 3822 cm^{-1} is due to the H_2 trapped in the hydrogen decorated divacancy $V_2 H_6$. In this case, the H_2 molecule is not at the center of vacant sites. It is dislodged from one of the vacant sites along $\langle 001 \rangle$ direction by 2.4 Å. The molecular axis is almost parallel to $\langle 110 \rangle$ direction (Fig. 4).

3.3 Oxygen incorporation

Finally, we consider oxygen incorporation of the vacancies. We determine the stable structures oxygen incorporated vacancies up to hexavacancy V_6 assuming that interstitial oxygen atom

Table 1: Calculated bond lengths d (Å) and vibration frequencies ω (cm^{-1}) of H_2 molecule at various locations. The anharmonic correction is shown in the parentheses.

	d (Å)	ω (cm^{-1})
Vacuum	0.739	4077 (-380)
T_d interstitial	0.767	3475 (-185)
VH_4	0.761	3583 (-260)
V_2H_6	0.746	3834 (-379)
V_6H_{12}	0.738	4008 (-444)
$V_{10}H_{16}$	0.739	4042 (-393)
Experiment		^a 3618, ^b 3822, ^c 4158

^aReference 13.

^bReference 5.

^cReference 14.

O_i diffuse in the crystal and then incorporated in the formally generated vacancy: We calculate the binding energy E_{bind} for the reaction of oxygen incorporation,

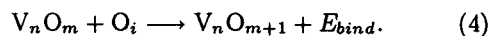


Table II shows the energy gains upon oxygen incorporation for V_n ($3 \leq n \leq 6$). In most case, it is found that an oxygen atom favors being trapped in the vacancy rather than being at the interstitial site. In each oxygen incorporated vacancies, an oxygen atom bridges two Si atoms which are nearest neighbors of the vacant sites. For the stable structures of oxygen incorporated vacancies, since V_6 is a stable negative cluster in Si, we predict that $V_6 O_6$ where each oxygen atom is bonded with a pair of Si neighbors of each vacant site is a stable oxygen incorporated negative cluster: each of 6 oxygen atoms bridges two nearest neighbor Si atoms of each vacant site in V_6 .

It is expected that the local vibration modes of stable oxygen incorporated vacancies are observed in IR absorption or Raman scattering experiments. We calculate vibration frequencies of $V_6 O_6$ by diagonalizing the dynamical matrix. The calculated vibration frequencies indicate the possibility that the $V_6 O_6$ is identified by means of IR or Raman experiments: the six higher frequencies of $V_6 O_6$ lying at 893~895 cm^{-1} , which correspond to asymmetric stretching vibration modes in which each oxygen atom vibrates almost parallel to $\langle 110 \rangle$ direction, are very close to the value of $V_1 O_1$ at 894 cm^{-1} , but lower frequencies of $V_6 O_6$ lying at 581~584 cm^{-1} , which correspond to symmetric stretching type vibration modes, are higher than the value of $V_1 O_1$ at 541 cm^{-1} ¹⁵⁾. We find that the difference in frequencies of symmetric type modes is interpreted by the interaction with the other oxygen atoms as well as the Si-O-Si bond angle: the charge redistribution around oxygen atom which presumably enhances the strength of Si-O-Si bond, and the decrease of the bond angle, may induce upward shift of frequencies. In $V_6 O_6$, we see that the upward shift of frequencies

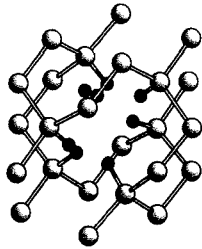


Figure 4: Atomic configuration of the H_2 molecule trapped in hydrogen decorated divacancy V_2H_6 . Large and small circles represent Si and H atoms, respectively. The H_2 molecule is located 2.4 Å above the vacant site (left vacant site in this atomic configuration).

Table 2: Calculated binding energies E_{bind} for oxygen incorporation of V_n ($3 \leq n \leq 6$).

Reactants	→	Product	E_{bind} (eV)
$V_3 + O_i$	→	V_3O_1	1.62
$V_3O_1 + O_i$	→	V_3O_2	1.79
$V_3O_2 + O_i$	→	V_3O_3	1.84
$V_3O_3 + O_i$	→	V_3O_4	0.51
$V_4 + O_i$	→	V_4O_1	1.88
$V_4O_1 + O_i$	→	V_4O_2	1.69
$V_4O_2 + O_i$	→	V_4O_3	1.79
$V_4O_3 + O_i$	→	V_4O_4	1.96
$V_4O_4 + O_i$	→	V_4O_5	0.60
$V_5 + O_i$	→	V_5O_1	2.68
$V_5O_4 + O_i$	→	V_5O_5	1.45
$V_6 + O_i$	→	V_6O_1	1.86
$V_6O_5 + O_i$	→	V_6O_6	1.50

for symmetric type modes mainly come from the Si-O-Si bond angle (145° for V_6O_6 , and 153° for V_1O_1).

4. SUMMARY

We have investigated the stable sizes and structures, and hydrogen and oxygen incorporation of the negative Si clusters. We have found the peculiar features of the electronic structure for stable negative clusters, which involve the relaxation of surrounding atoms generated by the negative cluster. We have also found that hydrogen and oxygen are capable of being contained in these negative clusters, and these clusters exhibit peculiar vibration spectra.

REFERENCES

- [1] See, for instance, G. D. Watkins, "Deep Centers in Semiconductors", Ed. by S. T.

- Pantelides, (Gordon and Breach, New York, 1986) p 147.
- [2] G. D. Watkins and J. W. Corbett, Phys. Rev. **138**, A543 (1965).; J. W. Corbett and G. D. Watkins, Phys. Rev. **138**, A555 (1965).
- [3] R. Car. P. J. Kelly, A. Oshiyama, and S. T. Pantelides, Phys. Rev. Lett. **52**, 1814 (1984).
- [4] D. J. Chadi and K. J. Chang, Phys. Rev. B **38**, 1523 (1988).
- [5] K. Ishioka *et al.*, Phys. Rev. **B60**, 10852 (1999).
- [6] D. M. Ceperley and B. J. Alder, Phys. Rev. Lett. **45**, 566 (1980); J. P. Perdew and A. Zunger, Phys. Rev. **B23**, 5048 (1981).
- [7] J. P. Perdew *et al.*, Phys. Rev. **B46**, 6671 (1992); J. P. Perdew, K. Burke, and M. Ernzerhof, Phys. Rev. Lett. **77**, 3365 (1996).
- [8] P. Hohenberg and W. Kohn, Phys. Rev. **136**, B864 (1964); W. Kohn and L. J. Sham, Phys. Rev. **140**, A1133 (1965).
- [9] N. Troullier and J. L. Martins, Phys. Rev. **B43**, 1993 (1991).
- [10] D. Vanderbilt, Phys. Rev. **B41**, (1990) 7892.
- [11] O. Sugino and A. Oshiyama, Phys. Rev. Lett. **68**, 1858 (1992).
- [12] In the calculation of oxygen incorporation, we use the plane-wave basis set with a cutoff energy of 22Ry.
- [13] R. E. Pritchard *et al.*, Phys. Rev. **B56**, 13118 (1997).
- [14] K. Murakami *et al.*, Phys. Rev. Lett. **77**, 3161 (1996).
- [15] T. Akiyama and A. Oshiyama, in *Proc. 25th Int. Conf. Physics of Semiconductors*, edited by N. Miura and T. Ando (Springer-Verlag, New York, 2001) p1425.

(Received December 28, 2001; Accepted January 28, 2002)